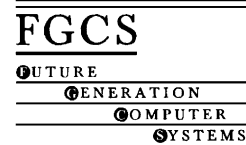




ELSEVIER

Future Generation Computer Systems 857 (2002) 1–13



www.elsevier.com/locate/future

MinEX: a latency-tolerant dynamic partitioner for grid computing applications

Sajal K. Das^{a,1}, Daniel J. Harvey^b, Rupak Biswas^{c,*}

^a Department of Computer Science and Engineering, The University of Texas at Arlington, GPO Box 13886, Arlington, TX 76019, USA

^b Department of Computer Science, Southern Oregon University, Ashland, OR 97520, USA

^c NASA Advanced Supercomputing Division, NASA Ames Research Center, Moffett Field, CA 94035, USA

Abstract

The information power grid (IPG) being developed by NASA is designed to harness, the power of geographically distributed computers, databases, and human expertise, in order to solve large-scale realistic computational problems. This type of a metacomputing infrastructure is necessary to present a unified virtual machine to application developers that hides the intricacies of a highly heterogeneous environment and yet maintains adequate security. In this paper, we present a novel latency-tolerant partitioning scheme, called MinEX, that dynamically balances processor workloads while minimizing data movement and runtime communication, for applications that are executed in a parallel distributed fashion on the IPG. The number of IPG nodes, the number of processors per node, and the interconnect speeds are parameterized in a simulation experiment to derive conditions under which the IPG would be suitable for solving such applications. Experimental results demonstrate that MinEX is an effective load balancer for the IPG when the nodes are connected by a high-speed asynchronous interconnection network. © 2002 Published by Elsevier Science B.V.

Keywords: Information power grid; Adaptive computations; Partitioning; Dynamic load balancing; Latency tolerance

1. Introduction

NASA and its collaborative partners are actively developing the information power grid (IPG) [20] to harness the vast collection of their geographically distributed resources (computers, databases, and human expertise). Current engineering and research status of the IPG project is available at <http://www.ipg.nasa.gov>. One of the primary benefits of the IPG will be to facilitate the efficient solution of large-scale computational problems by providing a scalable, adaptive, and transparent

environment that is both ubiquitous and uniformly accessible through a convenient interface. Some other areas that would benefit from such a nationwide infrastructure include:

- desktop coupling to remote resources so as to provide access to large data-bases and high-end graphics facilities [10];
- user access to sophisticated instruments through remote connections utilizing virtual reality techniques [9];
- Remote interactions with parallel and distributed supercomputer simulations [11,12].

The IPG is one of the several approaches to develop what are called *Computational Grid*² (in short, Grid)

* Corresponding author. Tel.: +1-650-604-4411;

fax: +1-650-604-3957.

E-mail addresses: das@cse.uta.edu (S.K. Das), harveyd@sou.edu (D.J. Harvey), rbiswas@nas.nasa.gov (R. Biswas).

¹ Tel.: +1-817-272-7405; fax: +1-817-272-3784.

² Not to be confused with computations on discretization grids.

46 capabilities and/or implementations [16]. For exam-
47 ple, Condor [23] was an early success in developing a
48 distributed system to manage research studies at work-
49 stations around the world. However, it does not ade-
50 quately deal with the security issues that are important
51 for a general Grid implementation. Other Grid-based
52 systems include Nimrod [1], NetSolve [4], NEOS [6],
53 Legion [17], and CAVERN [22]. The Globus Meta-
54 computing Infrastructure Toolkit [15] has been ex-
55 tremely successful in providing a portable virtual ma-
56 chine environment. Mechanisms exist within Globus
57 to share remote resources, provide adequate security,
58 and allow MPI-based message passing. Due to its gen-
59 eral, portable, and modular nature, Globus has been
60 chosen by NASA as the middleware to implement the
61 IPG.

62 Till date, only a few limited studies have been per-
63 formed at NASA Ames Research Center to determine
64 the viability of large-scale parallel and distributed
65 computing on the IPG [2,13]. In [2], latency tolerance
66 and load balancing modifications were implemented
67 for a computational fluid dynamics (CFD) applica-
68 tion to compensate for the slower communication
69 speed between two IPG computers (nodes). Results
70 showed that the application actually ran faster under
71 Globus on two nodes of four processors each than on
72 a single tightly coupled machine of eight processors.
73 However, this result is clouded in that asynchronous
74 message passing was supported over the wide area
75 network but not within the single platform. The re-
76 sults presented in [13] demonstrated the feasibility of
77 parallel distributed computing on homogeneous IPG
78 testbeds, but performance was significantly affected
79 by increased communication times. The paper con-
80 cluded that poorer connectivity and larger latencies
81 due to geographical separation in a realistic IPG en-
82 vironment could further impact overall performance.

83 With a goal to make more informative conclusions
84 regarding the latency tolerance and load balancing
85 performance of parallel distributed computational ap-
86 plications on the IPG, in this paper, we simulate an
87 unsteady adaptive mesh problem on a wide area net-
88 work. The number of nodes, the number of processors
89 per node, and the interconnect speeds between nodes
90 are all parameterized to derive general conditions un-
91 der which such an infrastructure would be suitable for
92 parallel distributed processing of this class of applica-
93 tions.

94 In our previous work, we have developed two dif-
95 ferent load balancing techniques for dynamic irregu-
96 lar applications. The first strategy, called PLUM [25],
97 is an architecture-independent framework which glob-
98 ally partitions the computational mesh after each adap-
99 tation and determines whether rebalancing the work-
100 load would reduce the total execution time. If an im-
101 provement in the load balance can be achieved, PLUM
102 utilizes one of several remapping algorithms to min-
103 imize the required data movement. Application pro-
104 cessing is temporarily suspended during the partition-
105 ing and data remapping operations. Utilization of a
106 parallel graph partitioner like ParMetis [21] gives ex-
107 tremely effective results.

108 The second approach, called symmetric broad-
109 cast networks (SBNs) [7], gives a general-purpose
110 topology-independent solution to dynamic load bal-
111 ancing. A salient feature of the SBN-based method
112 is that it balances processor workloads while the ap-
113 plication is running. Therefore, it is able to hide the
114 high data migration overhead, albeit at the cost of
115 increased interprocessor communication. Results re-
116 ported in [3] indicate that both PLUM and SBN have
117 their relative merits, and that they achieve excellent
118 load balance with minimal extra overhead.

119 In this paper, we propose a novel partitioner, called
120 MinEX, that optimizes the two important steps of
121 PLUM (namely, balancing and remapping) as part
122 of the partitioning process. Instead of attempting to
123 merely balance the load and reduce the runtime in-
124 terprocessor communication like most other partition-
125 ers, the objective of MinEX is to minimize the to-
126 tal runtime of the application. This approach coun-
127 ters the possibility that perfectly balanced loads with
128 minimal communication can still incur excessive re-
129 distribution costs for adaptive applications. MinEX is
130 also used to experiment with latency tolerant tech-
131 niques for the IPG. Our experimental results show that
132 MinEX reduces the workload migrated by PLUM, and
133 lowers the communication cost over partitions gener-
134 ated by SBN. For example, for 32 partitions with our
135 test case, PLUM showed an edge cut (reflecting the
136 communication overhead) of 10.9% and redistributed
137 63,270 mesh elements. The corresponding numbers
138 for the SBN-based approach were 36.5% and 19,446.
139 In contrast, the MinEX partitioner values were 20.9%
140 and 30,548, respectively, while maintaining compar-
141 able load balance. Thus, MinEX attempts to optimize

142 both communication and remapping costs, and can be
 143 an effective latency hiding technique in dynamic load
 144 balancing for Grid computing applications. A prelim-
 145 inary version of this paper appeared in Ref. [8].

146 The remainder of this paper is organized as follows.
 147 Section 2 introduces the dynamic irregular computa-
 148 tional application used as the test case for our exper-
 149 iments, and describes the various graphs and metrics
 150 that model the problem. Section 3 presents the new
 151 MinEX partitioner and gives implementation details.
 152 Performance results are reported and analyzed in Sec-
 153 tion 4. Finally, Section 5 summarizes our key conclu-
 154 sions as to the viability of MinEX and the IPG for this
 155 class of applications.

156 2. Preliminaries

157 In this section, we describe our computational test
 158 case, and the various graphs and metrics utilized to
 159 model the problem and evaluate MinEX.

160 2.1. Computational test case

161 Many computational problems are often modeled
 162 discretely as an unstructured mesh of vertices and
 163 edges. To capture evolving features, the mesh topol-
 164 ogy is also frequently adapted. For an efficient par-
 165 allel implementation, this requires dynamic load bal-
 166 ancing in the sense that mesh objects usually have
 167 to be reassigned after each adaptation phase to rebal-
 168 ance the workload among the processors. It is critical
 169 to minimize the overhead associated with remapping
 170 data sets, and to reduce the communication between
 171 processors during the subsequent solution step. These
 172 goals are particularly important in the context of the
 173 IPG where communication bandwidth between nodes
 174 are likely to be much smaller than those within a sin-
 175 gle node (i.e., multiprocessor machine).

176 The computational mesh considered for our exper-
 177 iments in this paper simulates an unsteady environment
 178 with a strongly time-dependent adapted region. As de-
 179 picted in Fig. 1, a shock wave is propagated through
 180 an initial tetrahedral grid to produce the desired effect.
 181 This grid is processed through nine adaptations by
 182 moving a cylindrical volume across the domain with
 183 constant velocity. Grid elements within the cylindrical
 184 volume are refined, while previously refined elements

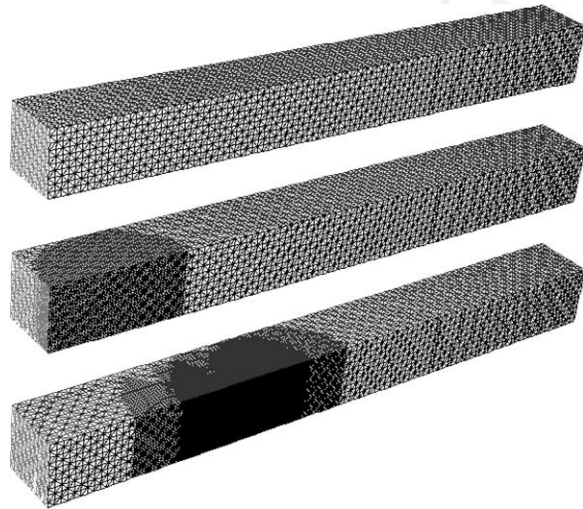


Fig. 1. Initial and adapted meshes (after levels 1 and 5) for the simulated experiment.

are coarsened in its wake. During the processing, the
 size of the mesh increases from 50,000 elements to
 1,833,730 elements.

2.2. Graph models

In our experiments, a dual graph representation of
 the initial mesh is used for load balancing where each
 original tetrahedron is a vertex of the graph. An edge
 exists between two dual graph vertices if the cor-
 responding elements share a face. Mesh refinement
 consists of subdividing parent tetrahedral elements
 into two, four, or eight subelements in specified re-
 gions of the mesh. Subsequent refinements can fur-
 ther split the child elements, thereby forming a re-
 finement tree of tetrahedra for each original mesh
 element.

To realistically simulate the overhead associated
 with such an adaptive mesh computation, weights are
 associated with the vertices and edges of the dual
 graph. Each vertex v has two weights, $Pwgt_v$ and
 $Rwgt_v$, while each edge (v, w) has one weight,
 $Cwgt_{(v,w)}$. These weights respectively model the as-
 sociated computational processing, data remapping,
 and runtime interprocessor communication costs. $Pwgt_v$
 is proportional to the number of leaves in the refine-
 ment tree because only those elements participate in
 the actual calculation. However, $Rwgt_v$ is propor-
 tional to

211 the total number of elements in the refinement tree be-
 212 cause the entire tree must be relocated when the root is
 213 reassigned to another processor. Finally, $Cwgt_{(v,w)}$ de-
 214 pends on the number of leaf faces between dual graph
 215 vertices v and w .

216 To predict performance on a variety of distributed
 217 architectures, a configuration graph is utilized. Each
 218 vertex in this fully connected graph represents a
 219 tightly coupled cluster of processors, while edges
 220 denote cluster interconnects. For the experiments re-
 221 ported here, we assume that all processors in a single
 222 cluster (node) are homogeneous and that there is
 223 a constant bandwidth for intra-cluster communica-
 224 tion. Vertex c in the configuration graph has weight
 225 $Proc_c \geq 1$ that represents the processing slowdown
 226 factor for the corresponding cluster. Similarly, the
 227 edge weight $Conn_{(c,d)} \geq 1$ represents the intercon-
 228 nect slowdown factor when a processor in cluster c
 229 communicates with a processor in another cluster d .
 230 If $c = d$, $Conn_{(c,c)}$ is the slowdown associated with
 231 communication between processors in the same clus-
 232 ter c . Note that if any of these weights are unity, there
 233 is no slowdown (ideal conditions).

234 2.3. Metrics

235 The following three metrics respectively measure
 236 the number of time units required for computation,
 237 communication, and remapping. The total time re-
 238 quired to process the elements assigned to processor
 239 p in cluster c must take into account all of them.

240 • *Processing cost:* Wgt_v^p is the computational cost to
 241 process dual graph vertex v assigned to processor p
 242 which is in cluster c :

$$243 \quad Wgt_v^p = Pwgt_v \times Proc_c.$$

244 • *Communication cost:* $Comm_v^p$ is the communication
 245 cost to interact with all vertices w adjacent to v
 246 whose data sets are not local to p (assuming that v
 247 is assigned to p):

$$248 \quad Comm_v^p = \sum_w Cwgt_{(v,w)} \times Conn_{(c,d)},$$

249 where c and d are the clusters containing the pro-
 250 cessors to which v and w are respectively assigned.
 251 Obviously, if the data sets of all vertices adjacent to
 252 v are also assigned to p , then $Comm_v^p = 0$.

• *Redistribution cost:* $Remap_v^p$ is the overhead to copy 253
 the data set associated with v to another processor 254
 from p : 255

$$256 \quad Remap_v^p = Rwgt_v \times Conn_{(c,d)},$$

where c and d are the clusters containing the source 257
 and destination processors for v . Note that the redis- 258
 tribution cost incurred at p includes the operations 259
 of packing data and initiating transmission, while 260
 the cost incurred by the processor receiving v is 261
 the sum of the communication time and the cost of 262
 unpacking and merging the data into existing data 263
 structures. Clearly, $Remap_v^p = 0$ if the data set for 264
 v is already assigned to p . 265

Five additional metrics used in this work are defined 266
 below. 267

• *Weighted queue length:* $Qwgt^p$ is the total cost to 268
 process all vertices v assigned to p : 269

$$270 \quad Qwgt^p = \sum_v (Wgt_v^p + Comm_v^p + Remap_v^p).$$

• *Total system load:* $QwgtTot$ is the cost to process 271
 the entire application: 272

$$273 \quad QwgtTot = \sum_p Qwgt^p.$$

• *Heaviest load:* $MaxQwgt$ indicates the total time 274
 required to process the application: 275

$$276 \quad MaxQwgt = \max_p Qwgt^p.$$

• *Lightest load:* $MinQwgt$ indicates the workload of 277
 the most lightly loaded processor: 278

$$279 \quad MinQwgt = \min_p Qwgt^p.$$

• *Load imbalance factor:* $LoadImb$ represents the 280
 quality of the partitioning: 281

$$282 \quad LoadImb = P \times \frac{MaxQwgt}{QwgtTot},$$

where P is the total number of processors in the 283
 configuration graph. 284

285 3. MinEX: a new partitioner

286 Previous studies with the test application (described
287 in Section 2.1) under PLUM utilized a variety of
288 general-purpose partitioners such as ParMetis [21],
289 UAMetis [26], DAMetis [26], Jostle-MS [27], and
290 Jostle-MD [27]. Note that UAMetis, DAMetis, and
291 Jostle-MD are diffusive schemes designed to mod-
292 ify existing partitions to produce a processor allo-
293 cation, whereas ParMetis and Jostle-MS are global
294 from-scratch partitioners which make no assumptions
295 about the original distribution of the mesh. Although
296 all these partitioners achieve good load balance while
297 minimizing communication overhead, they fail to
298 consider the cost of moving data between proces-
299 sors. A unique feature of PLUM is to address this
300 drawback through the use of an efficient heuristic for
301 redistributing data to assigned processors.

302 In the following subsections, we design, implement,
303 and analyze a novel partitioner, called MinEX, that
304 optimizes computational, communication, and data
305 remapping costs. We also redefine the partitioning
306 goal from producing balanced workloads to minimiz-
307 ing the *MaxQwgt* metric. No direct comparisons with
308 other existing partitioners mentioned above were fea-
309 sible since MinEX also considers the data redistribu-
310 tion cost while partitioning the computational mesh.

311 3.1. General design principles

312 MinEX can be classified as a diffusive multilevel
313 partitioner. Diffusive algorithms [5] utilize an exist-
314 ing partition as a starting point instead of partitioning
315 from scratch. The multilevel approach, originally in-
316 troduced in [19], partitions a graph into three steps:
317 contraction, partitioning, and expansion—each of
318 which is described below.

319 Similar to other multilevel partitioners, the first step
320 in MinEX is to contract the mesh to a reasonable size.
321 However, instead of repeatedly contracting the mesh in
322 halves as is common with other multilevel partitioners,
323 MinEX sequentially contracts one vertex at a time.
324 The advantage of this approach is that a decision can
325 be made each time and a vertex is later refined as to
326 whether it should be assigned to another processor.
327 This makes the algorithm more flexible since the graph
328 does not have to be doubled in size before this decision
329 could be made. If $|V|$ is the number of vertices in

the mesh, the contraction step requires $O(|V|)$ substeps 330
which is asymptotically equal to the complexity of 331
contracting the mesh sequentially in halves. 332

Once the mesh is sufficiently contracted, the re- 333
maining vertices are reassigned according to the par- 334
titioning criteria described in Section 3.3. 335

Finally, the mesh is expanded back to its original 336
size through a refinement process. As each vertex is 337
reinstated, a decision is made as to whether or not it 338
should be reassigned. This decision employs the same 339
criteria as used by the partitioning algorithm. Note that 340
each coarse vertex reassignment, in effect, reassigns 341
all of the original dual graph vertices that the coarse 342
vertex represents. 343

344 3.2. Latency tolerance

Our MinEX partitioner can interact via a user- 345
defined function to accommodate any latency tol- 346
erance that a mesh application may possess. The 347
following steps illustrate how the application can be 348
programmed so that MinEX eliminates (or at least 349
reduces) communication and data redistribution costs. 350

- Step 1 Initiate send of all computational data sets that 351
are to be redistributed to other processors. 352
- Step 2 For each edge (v, w) , where the data set for 353
vertex v is local to processor p and the data 354
set for vertex w is local to another processor 355
 q , initiate send of communication data. Also 356
initiate send of communication data needed by 357
adjacent processors. 358
- Step 3 Process vertices that are not waiting for any 359
incoming transmissions. 360
- Step 4 Receive and unpack any remapped computa- 361
tional data sets destined for processor p . 362
- Step 5 Receive and unpack communication data des- 363
tined for this processor. 364
- Step 6 Repeat Steps 2–5 until all vertices are pro- 365
cessed. 366

These steps implement a strategy where processors 367
distribute computational and communication data as 368
early as possible. Internal vertices can then be ser- 369
viced while waiting for expected incoming messages. 370
As information is received, additional communica- 371
tions can be initiated and vertices processed. The most 372
optimistic view of this strategy is that the processing 373
activity can entirely hide the data redistribution cost 374

375 and communication latency. At the other extreme, the
 376 most pessimistic view is that no latency tolerance is
 377 achieved. To analyze the effect of latency tolerance
 378 on our test application, experiments simulating both
 379 possibilities are described in Section 4.

380 3.3. Partitioning criteria

381 The criteria for deciding whether a vertex should be
 382 reassigned from one processor to another is based on
 383 two metrics: *Gain* and *MinVar*. These are obtained as
 384 follows:

- 385 • *Gain* represents the change in *QwgtTot* that would
 386 result from a proposed vertex move. A negative
 387 value indicates that less total processing is required
 388 after such a vertex reassignment. The partitioning
 389 algorithm favors vertex moves with negative
 390 or small *Gain* values that reduce or minimize the
 391 overall system load.
- 392 • *MinVar* measures the variance of processor work-
 393 loads from that of the most lightly loaded processor.
 394 It is computed using the workload for each proces-
 395 sor p and the smallest load over all processors:

$$MinVar = \sum_p (Qwgt^p - MinQwgt)^2.$$

397 The objective is to initiate vertex moves that lower
 398 this value. Since processors with large $Qwgt^p$ val-

399 ues will have large *MinVar* components, this
 400 criteria tends to move vertices away from processors
 401 that have high runtime requirements. $\Delta MinVar$ is
 402 the change in *MinVar* after moving a vertex from
 403 one processor to another. A negative value indicates
 404 that *MinVar* has been reduced.

405 The partitioning decisions are made as follows. For
 406 each vertex v , consider all adjacent vertices assigned
 407 to other processors. Compute the *Gain* and *MinVar*
 408 values that would result from moving v to each of
 409 these adjacent processors. The vertex moved is the one
 410 with the smallest *Gain*, and satisfies $\Delta MinVar < 0$
 411 and $-Gain/\Delta MinVar < ThroTtle$, where *ThroTtle* is
 412 a user-supplied parameter. To increase efficiency, we
 413 use a minimum heap with pointers to vertex locations
 414 in order to rapidly find the best migration and directly
 415 remove entries without searching.

416 Conceptually, *ThroTtle* acts as a gate that limits in-
 417 creases in *Gain* based upon how much of an improve-
 418 ment in *MinVar* can be achieved. Table 1 shows how
 419 varying *ThroTtle* affects the expected application run-
 420 time (*MaxQwgt*) and load balance quality (*LoadImb*),
 421 assuming maximum latency tolerance. The *MaxQwgt*
 422 entries are non-dimensionalized values in thousands,
 423 and were obtained by running the experiments de-
 424 scribed in Section 4. Table 1 results are for a network
 425 of $P = 32$ homogeneous processors distributed over
 426 1–8 IPG nodes (clusters). The inter-cluster intercon-

Table 1
 Expected runtime and load balance quality with maximum latency tolerance for varying *ThroTtle* values and $P = 32$

Metric	Clusters	<i>ThroTtle</i> values							
		0	1	4	16	32	64	128	∞
<i>MaxQwgt</i>	1	1993	1427	312	291	300	306	312	324
	2	1847	1142	467	320	304	305	318	345
	3	2035	1801	556	375	331	324	326	382
	4	1868	1516	639	412	352	328	371	425
	5	1834	1626	767	438	373	359	343	400
	6	2081	1579	825	481	391	357	361	427
	7	1884	1279	758	505	383	371	369	414
	8	1944	1451	834	531	434	376	380	435
<i>LoadImb</i>	1	7.05	5.09	1.11	1.01	1.00	1.00	1.00	1.00
	2	8.54	4.16	1.81	1.26	1.14	1.04	1.00	1.00
	3	7.15	6.40	2.11	1.41	1.19	1.05	1.02	1.01
	4	6.63	5.41	2.40	1.58	1.26	1.07	1.03	1.01
	5	6.53	5.78	2.83	1.66	1.30	1.11	1.02	1.01
	6	7.31	5.58	2.99	1.81	1.40	1.08	1.02	1.01
	7	6.68	4.61	2.80	1.84	1.33	1.10	1.03	1.00
	8	6.90	5.15	3.05	1.94	1.43	1.13	1.06	1.00

nect speed is assumed to be a third of the intra-cluster
 speed. Observe that $ThroTTle = 64$ produces the low-
 est overall $MaxQwgt$, and that larger $ThroTTle$ values
 improve $LoadImb$. Experiments with other network
 sizes using these same application have shown that
 $ThroTTle$ generally converges at values between P and
 $2P$. Note also that for large values of $ThroTTle$, better
 $LoadImb$ does not necessarily imply lower $MaxQwgt$.

3.4. Data structures

We give here a brief description of the data struc-
 tures used for implementing the multilevel MinEX
 partitioner:

Mesh. The adaptive mesh, represented as $\{|V|, |E|, vTot, *VMap, *VList, *EList\}$, where $|V|$ is the number of active vertices, $|E|$ the number of edges, $vTot$ the total vertex count (including merged vertices), $*VMap$ is a pointer to the list of active vertices, $*VList$ is a pointer to the complete list of vertices, and $*EList$ is a pointer to the list of edges.

VMap. The list of active vertices (those that have not been compressed during multilevel partitioning).

VList. The complete list of vertices. Each vertex v is represented as $\{Pwgt_v, Rwgt_v, |e|, *e, merge, lookup, *vmap, *Heap, border\}$, where $Pwgt_v$ is the computational cost to process v , $Rwgt_v$ the redistribution cost to copy the data set associated with v , $|e|$ the number of edges incident on v , $*e$ is a pointer to the first incident edge (subsequent edges are stored contiguously), $merge$ the vertex that was merged with v during a contraction operation (set to -1 if not merged), $lookup$ is the active vertex that contains v after a series of contractions (set to -1 if not merged), $*vmap$ is a pointer to the position of v in $VMap$, $*Heap$ is a pointer to v 's heap entry and represents a potential reassignment of v , and $border$ is a boolean flag indicating whether v is adjacent to vertices assigned to other processors.

EList. The list of edges in the mesh. Each vertex v in $VList$ points to its first edge in $EList$ using $*e$. Each edge record is defined as $\{w, Cwgt_{(v,w)}\}$, where w is a vertex adjacent to v and $Cwgt_{(v,w)}$ the communication weight associated with this edge.

Heap. The heap of potential vertex reassignments. Each heap record is defined as $\{Gain, \Delta MinVar, v, p\}$ which specifies the $Gain$ and $\Delta MinVar$ that

would result from reassigning vertex v to processor p . The min-heap is keyed by the $Gain$ value. *Stack*. The stack of collapsed edges (v, w) . These pushed edges are refined in an order reversed from the one in which they were compressed. This graph contraction technique is described in the next section.

3.5. Graph contraction

MinEX randomly selects a set of adjacent vertex pairs that are assigned to the same processor. From this set, the vertex pair (v, w) that has the largest $Cwgt_{(v,w)}/(Rwgt_v + Rwgt_w)$ value is merged. This formula attempts to find edges with large communication costs while minimizing the potential data redistribution overhead. The motivation behind this strategy is to arrive at a contracted mesh with a small edge cut as well as a small data distribution cost.

To collapse the edge (v, w) , a merged vertex M is generated. The edges incident on M are created by utilizing the edge lists of vertices v and w . $VMap$ is adjusted to contain M and to remove v and w ; $|V|$ is decremented and $vTot$ is incremented; $|E|$ is increased by the number of edges created for M ; and the pair (v, w) is pushed onto *Stack*. The entire process is repeated until the graph is sufficiently contracted.

This contraction procedure is implemented using a set Union/Find algorithm so that edges of unmerged vertices remain unchanged. For example, if an unmerged vertex is adjacent to v , accesses to its *EList* will check whether v has been merged. If it has, *lookup* will quickly find the appropriate merged vertex. If *lookup* is not current (i.e., $lookup > vTot$), the Union/Find algorithm will search the chain of vertices beginning with *merge* in order to update *lookup*, so that subsequent queries can be done efficiently. The pseudo-code describing the Union/Find procedure is given in Fig. 2.

3.6. Partitioning the contracted graph

The partitioning is performed when the graph contraction process is complete. MinEX partitioning is efficient because the number of vertices is greatly reduced. The algorithm considers every vertex of the coarse mesh to find potential reassignments that will reduce $Gain$ and $MinVar$ as described in Section 3.3. All potential vertex reassignments are added to the

```

procedure Find (v)
if (merge = -1) return (v)
if ((lookup ≠ -1) and (lookup ≤ vTot))
  then return (lookup = Find (lookup))
  else return (lookup = Find (merge))

```

Fig. 2. Pseudo-code for the Union/Find algorithm.

516 min-heap, and executed in heap order. After each re-
 517 assignment, the heap is adjusted to reflect the new par-
 518 tition.

519 3.7. Graph expansion

520 The graph is restored to its original size by ex-
 521 panding pairs of vertices in an order reversed from
 522 which they were merged. The *Stack* data structure con-
 523 trols the order. As pairs of vertices (*v*, *w*) are refined,
 524 merged edges and vertices are deallocated. The *merge*
 525 and *lookup* values are also adjusted in *VList*. The list
 526 *VMap* of active vertices is updated to delete the merged
 527 vertex *M*, and to add *v* and *w*; $|V|$ is incremented and
 528 *vTot* is decremented; and $|E|$ is decreased by the num-
 529 ber of edges created for *M*. After each refinement, it
 530 is checked whether a partition can be improved by re-
 531 assigning *v* or *w*. When reassignments are made, ad-
 532 jacent border vertices are also considered.

533 4. Performance results

534 In the experimental study presented below, two ex-
 535 treme cases are considered. The first is the most opti-
 536 mistic view in which processing activity can entirely
 537 hide the data set redistribution and communication la-
 538 tency. The second case, on the other hand, is the most
 539 pessimistic view where no latency tolerance can be
 540 achieved.

541 The MinEX partitioner was executed with the com-
 542 putational test case (described in Section 2.1) that
 543 simulates an adaptive mesh calculation. A variety of
 544 system configurations was evaluated. Individual runs
 545 model networks with varying number of processors
 546 (*P*), number of IPG nodes/clusters (*C*), *ThroTTle* val-
 547 ues, and interconnect slowdowns (*I*). In our experi-
 548 ments, *P* ranged from 2 to 2048, *C* from 1 to 8, *ThroT-*
 549 *Tle* was varied to find the optimal value for minimiz-

ing runtime, and *I* simulated high- and low-bandwidth
 cluster interconnections.

550
 551
 552 Based on performance studies reported in [14,24],
 553 typical communication latencies and bandwidth slow-
 554 downs from integrated clusters to configurations con-
 555 nected through a high-speed interconnect are in the
 556 range 3–100. Wide area network connections are typ-
 557 ically 1000–10,000 times slower than the internal in-
 558 traconnects of a single cluster. In our experiments, we
 559 normalized the intra-cluster communication speed to
 560 unity. Simulations of inter-cluster communication as-
 561 sumed slowdown factors of 3, 10, 100, and 1000. To
 562 simplify the analysis, we also assumed that individual
 563 processors are homogeneous and divided as evenly as
 564 possible among the clusters.

565 Table 2 shows results of experimental runs analyz-
 566 ing the effect of varying numbers of clusters and inter-
 567 connect speeds, for $P = 32$ homogeneous processors
 568 and *ThroTTle* = 64. The interconnect speeds indicate
 569 the slowdown factor relative to the intra-cluster com-
 570 munication speed. Results are presented both when
 571 no latency tolerance is achieved, and also with maxi-
 572 mum latency tolerance. To be consistent with Table 1,
 573 runtimes are shown as non-dimensionalized values in
 574 thousands. The following conclusions can be drawn
 575 from these experiments.

576 As the interconnect speed is reduced, the slowdown
 577 experienced by utilizing additional clusters increases
 578 dramatically. For example, the runtime metric with no
 579 latency tolerance as shown in Table 2 is 4102 when
 580 two clusters and an interconnect slowdown of 1000
 581 is assumed; however, the metric is 93,566 when eight
 582 clusters are assumed. Thus, performance deteriorates
 583 by almost a factor of 22.8. Instead, if we consider an
 584 interconnect slowdown of 3, the performance degra-
 585 dation is only 1.3. The same pattern also holds true
 586 when maximum latency tolerance is assumed.

587 We can compare the effectiveness of latency tol-
 588 erant algorithms to those without latency tolerance

Table 2
Expected runtime (*MaxQwgt*) without and with latency tolerance for varying interconnect slowdowns, $P = 32$, and *ThroTTle* = 64

Case	Clusters	Interconnect slowdowns			
		3	10	100	1000
No latency tolerance	1	507	507	507	507
	2	728	863	1228	4102
	3	755	1168	2783	18512
	4	791	1361	3667	25040
	5	854	1649	5677	53912
	6	915	1717	8521	76169
	7	956	1915	10958	80568
	8	968	2178	11492	93566
Maximum latency tolerance	1	306	306	306	306
	2	305	469	763	3941
	3	324	548	2386	12705
	4	328	680	3297	21888
	5	359	768	4369	33092
	6	357	856	5044	52668
	7	371	893	5480	61079
	8	376	1048	5721	61321

Table 3
Expected runtime and load balance quality without and with latency tolerance for varying number of processors, $I = 3$, and *ThroTTle* = $2P$

Case	Processors	<i>MaxQwgt</i>		<i>LoadImb</i>		
		$C = 1$	$C = 8$	$C = 1$	$C = 8$	
No latency tolerance	2	4526		1.00		
	4	2922		1.00		
	8	1568	2518	1.00	1.01	
	16	910	1493	1.00	1.17	
	32	507	968	1.01	1.48	
	64	276	563	1.05	1.69	
	128	169	405	1.19	2.42	
	256	131	253	1.66	2.80	
	512	111	214	2.47	4.69	
	1024	105	214	4.16	8.95	
	2048	102	170	7.47	14.33	
	Maximum latency tolerance	2	3782		1.00	
		4	2014		1.00	
8		1089	1245	1.00	1.00	
16		589	661	1.00	1.00	
32		306	376	1.00	1.13	
64		158	246	1.01	1.39	
128		85	176	1.05	1.98	
256		73	124	1.60	2.77	
512		61	103	2.47	4.14	
1024		55	95	4.04	7.79	
2048		60	86	8.14	13.43	

589 by measuring runtimes of each approach as the number
 590 of clusters and interconnect speeds are varied.
 591 The performance improvements using latency toler-
 592 ance increase dramatically as the number of clusters
 593 increases. This can be verified by comparing corre-
 594 sponding rows in Table 2. For example, consider the
 595 results with eight clusters. The runtime improvements
 596 comparing latency tolerant algorithms to those with
 597 no latency tolerance are factors of 2.7, 2.1, 2.0, and
 598 1.5, respectively, for interconnect slowdowns of 3, 10,
 599 100, and 1000. In contrast, results with two clusters
 600 indicate gains of 2.4, 1.8, 1.6, and 1.0, respectively,
 601 for the same interconnect slowdowns. These results
 602 clearly demonstrate that utilizing more clusters give
 603 greater runtime improvement when employing latency
 604 tolerance.

605 The same is also true when the interconnect slow-
 606 downs are varied (this can be analyzed by comparing
 607 the corresponding columns in Table 2). For example,
 608 with an interconnect slowdown of 1000, the runtime
 609 improvement factors when utilizing latency tolerance
 610 are 1.6, 1.0, 1.5, 1.1, 1.6, 1.4, 1.3, and 1.5, respec-
 611 tively, for 1–8 clusters. On the other hand, with an

interconnect slowdown of 10, the corresponding factors
 are 1.6, 1.8, 2.1, 2.0, 2.1, 2.0, 2.1, and 2.1. In this
 case, results somewhat surprisingly demonstrate that
 latency tolerance has a bigger payoff when intercon-
 nect slowdowns are smaller. Additional investigations
 are required to verify/counter this observation.

For our class of applications, the IPG could be a vi-
 able environment if a high-speed interconnect (slow-
 down factor between 3 and 10) between clusters is
 available. Results in Table 2 comparing 1 and 8 clus-
 ters with an interconnect slowdown of 3 show runtime
 deterioration factors of 1.24 and 2.04 with and with-
 out latency tolerance, respectively. Similar compar-
 isons for an interconnect slowdown of 10 show deteri-
 oration factors of 3.65 and 4.60. These factors, being
 smaller than the number of clusters, indicate a relative
 speedup when the number of clusters increases.

Table 3 presents simulation results when the total
 number of processors P is varied, for interconnect
 slowdown $I = 3$ and $ThroTtle = 2P$. Both the ex-
 pected runtime ($MaxQwgt$) and the load balance qual-
 ity ($LoadImb$) with and without latency tolerance are
 reported, but only for 1 and 8 clusters. The perfor-

Table 4
 Expected runtime and load balance quality without and with latency tolerance for varying number of processors, $I = 3$, $ThroTtle = 2P$, and no partitioning

Case	Processors	$MaxQwgt$		$LoadImb$		
		$C = 1$	$C = 8$	$C = 1$	$C = 8$	
No latency tolerance	2	6621		1.80		
	4	5434		2.57		
	8	3624	4712	2.81	2.70	
	16	2825	3739	3.22	3.34	
	32	1725	2207	3.37	3.45	
	64	964	1294	3.50	3.78	
	128	663	868	4.10	4.50	
	256	407	524	4.38	4.87	
	512	392	503	8.17	8.77	
	1024	353	431	13.54	13.45	
	2048	247	304	17.74	17.80	
	Maximum latency tolerance	2	6561		1.81	
		4	5125		2.63	
		8	3142	3142	2.97	2.95
16		1832	1910	3.10	3.05	
32		1036	1265	3.27	3.52	
64		560	776	3.41	3.93	
128		364	516	4.07	4.69	
256		205	328	4.24	5.35	
512		198	317	7.93	9.53	
1024		178	281	13.08	14.61	
2048	128	199	17.56	19.23		

mance ratio between the two cluster configurations remains roughly constant across all processor counts. So too does the ratio between maximum and zero latency tolerance. Note that generally near optimal results are obtained when *ThroTTle* is set to a value of $2P$; however, when $\text{ThroTTle} = 3P$ for $P = 1024$ and $C = 8$, *MaxQwgt* and *LoadImb* both improve to 188 and 7.22, respectively (compared to 214 and 8.95 as reported in Table 3).

Table 3 also demonstrates the scalability of our test application. The benefits of using more processors begins to decrease beyond $P = 128$ as is evident from the *MaxQwgt* values. The quality of load balance also deteriorates rapidly when $P > 256$. This is because the problem size for our test application does not increase with P but is fixed at 50,000 elements (see Section 2.1).

Finally, to evaluate the effectiveness of MinEX versus the case where no partitioning is done, additional experiments were conducted. These results are reported in Table 4 where the settings are identical to those in Table 3 except that the MinEX partitioner was not invoked. As expected, the quality of load balance is severely affected, even for small numbers of processors. The expected runtimes also increase by about a factor of 2. Other interconnect and cluster combinations showed significant improvements as well when using MinEX (but the results are not reported here due to length restrictions). For example, with $I = 100$ and $C = 4$, MinEX reduces the expected runtime from 17,752 to 3297 if maximum latency tolerance occurs. Similarly, if no latency tolerance is possible, the improvement in runtime is from 18,323 to 3667. In both cases, MinEX improves the runtime by approximately a factor of 5.

5. Conclusions

In this paper, we presented a novel latency-tolerant partitioner, called MinEX, that is suitable for adaptive mesh applications executed in a parallel distributed fashion on NASA's IPG. MinEX not only balances processor workloads but also minimizes data movement and runtime communication, and can account for expected latency tolerance in the application. Our simulation results demonstrated that MinEX is a viable load balancer provided the IPG nodes are con-

nected by a high-speed asynchronous interconnection network. Otherwise, applications would have to have little runtime communication and data set remapping overhead for low-speed wide area networks to be practical interconnects. For details on other applications, see [18]. Implementing a parallel version of MinEX and conducting a rigorous mathematical analysis are part of our future work. Finally, real distributed experiments using Globus are planned to complement the results presented in this paper.

Acknowledgements

The work of the first two authors was partially supported by NASA Ames Research Center under Cooperative Agreement No. NCC 2-5395.

References

- [1] D. Abramson, R. Sasic, J. Giddy, R. Hall, Nimrod: a tool for performing parametrised simulations using distributed workstations, in: Proceedings of the Fourth IEEE Symposium on High Performance Distributed Computing, Washington, DC, 1995, pp. 112–121.
- [2] S. Barnard, R. Biswas, S. Saini, R. Van der Wijngaart, M. Yarow, L. Zechter, Large-scale distributed computational fluid dynamics on the information power grid using Globus, in: Proceedings of the Seventh Symposium on the Frontiers of Massively Parallel Computation, Annapolis, MD, 1999, pp. 60–67.
- [3] R. Biswas, S.K. Das, D.J. Harvey, L. Oliker, Parallel dynamic load balancing strategies for adaptive irregular applications, *Appl. Math. Model.* 25 (2000) 109–122.
- [4] H. Casanova, J. Dongarra, NetSolve: a network server for solving computational science problems, *Int. J. Supercomputer Appl.* 11 (1997) 212–223.
- [5] G. Cybenko, Dynamic load balancing for distributed-memory multiprocessors, *J. Parallel Distributed Comput.* 7 (1989) 279–301.
- [6] J. Czyzyk, M.P. Mesnier, J.J. Moré, The network-enabled optimization system (NEOS) server, Preprint MCS-P615-1096, Argonne National Laboratory, Argonne, IL, 1996.
- [7] S.K. Das, D.J. Harvey, R. Biswas, Parallel processing of adaptive meshes with load balancing, *IEEE Trans. Parallel Distributed Syst.*, in press.
- [8] S.K. Das, D.J. Harvey, R. Biswas, Latency hiding in dynamic partitioning and load balancing of grid computing applications, in: Proceedings of the First International Symposium on Cluster Computing and the Grid, Brisbane, Australia, 2001, pp. 347–354.
- [9] T.A. DeFanti, M.D. Brown, R. Stevens, Virtual reality over high-speed networks, *IEEE Comput. Graphics Appl.* 16 (1996) 42–43.

- 729 [10] T.A. DeFanti, I. Foster, M.E. Papka, R. Stevens, T. Kuhfuss, 786
730 Overview of the I-way wide area visual supercomputing, Int. 787
731 J. Supercomputer Appl. 10 (1996) 123–130. 788
- 732 [11] D. Diachin, L. Freitag, D. Heath, J. Herzog, W. Michels, 789
733 P. Plassmann, Remote engineering tools for the design of 790
734 pollution control systems for commercial boilers, Int. J. 791
735 Supercomputer Appl. 10 (1996) 208–218.
- 736 [12] T.L. Disz, M.E. Papka, M. Pellegrino, R. Stevens, 786
737 Sharing visualization experiences among remote virtual 787
738 environments, in: Proceedings of the International Workshop 788
739 on High Performance Computing for Computer Graphics and 789
740 Visualization, Swansea, UK, 1995, pp. 217–237.
- 741 [13] M.J. Djomehri, R. Biswas, R.F. Van der Wijngaart, M. 790
742 Yarrow, Parallel and distributed computational fluid dynamics: 791
743 experimental results and challenges, in: Proceedings of 786
744 the Seventh International Conference on High Performance 787
745 Computing, Bangalore, India, 2000, Lecture Notes in 788
746 Computer Science, Springer, Berlin, 1970, pp. 183–193.
- 747 [14] I. Foster, N. Karonis, A grid-enabled MPI: message passing in 789
748 heterogeneous distributed computing systems, in: Proceedings 790
749 of the Supercomputing'98, Orlando, FL, 1998.
- 750 [15] I. Foster, C. Kesselman, Globus: a metacomputing 786
751 infrastructure toolkit, Int. J. Supercomputer Appl. 11 (1997) 787
752 115–128. Also at <http://www.globus.org>.
- 753 [16] I. Foster, C. Kesselman, The Grid: Blueprint for a New 788
754 Computing Infrastructure, Morgan Kaufmann, San Francisco, 789
755 CA, 1999.
- 756 [17] A. Grimshaw, W. Wulf, et al., The legion vision of a world- 790
757 wide virtual computer, Commun. ACM 40 (1997) 39–45.
- 758 [18] D.J. Harvey, Load balancing techniques for distributed 786
759 processing environments, Ph.D. Thesis, The University of 787
760 Texas at Arlington, Arlington, TX, 2001.
- 761 [19] B. Hendrickson, R. Leland, A multilevel algorithm for 788
762 partitioning graphs, Technical Report SAND93-1301, Sandia 789
763 National Laboratories, Albuquerque, NM, 1993.
- 764 [20] W.E. Johnston, D. Gannon, B. Nitzberg, Grids as production 790
765 computing environments: the engineering aspects of NASA's 786
766 information power grid, in: Proceedings of the Eight 787
767 International Symposium on High Performance Distributed 788
768 Computing, Redondo Beach, CA, 1999, pp. 197–204.
- 769 [21] G. Karypis, V. Kumar, Parallel multilevel k-way partitioning 789
770 scheme for irregular graphs, Technical Report 96-036, 790
771 University of Minnesota, Minneapolis, MN, 1996.
- 772 [22] J. Leigh, A.E. Johnson, T.A. DeFanti, CAVERN: a 786
773 distributed architecture for supporting scalable persistence and 787
774 interoperability in collaborative virtual environments, Virtual 788
775 Reality Res., Develop. Appl. 2 (1997) 217–237.
- 776 [23] M.J. Litzdow, M. Livny, M.W. Mutka, Condor—a hunter of 789
777 idle workstations, in: Proceedings of the Eight International 790
778 Conference of Distributed Computing Systems, San Jose, CA, 786
779 1988, pp. 104–111.
- 780 [24] S. Nog, D. Kotz, A performance comparison of TCP/IP and 787
781 MPI on FDDI, fast Ethernet, and Ethernet, Technical Report 788
782 PCS-TR95-273, Dartmouth College, Hanover, NH, 1996.
- 783 [25] L. Oliker, R. Biswas, PLUM: parallel load balancing for 789
784 adaptive unstructured meshes, J. Parallel Distributed Comput. 790
785 52 (1998) 150–177.
- [26] K. Schloegel, G. Karypis, V. Kumar, Multilevel diffusion 786
787 schemes for repartitioning of adaptive meshes, J. Parallel 788
789 Distributed Comput. 47 (1997) 109–124. 790
791
- [27] C. Walshaw, M. Cross, M. Everett, Parallel dynamic graph 786
787 partitioning for adaptive unstructured meshes, J. Parallel 788
789 Distributed Comput. 47 (1997) 102–108. 790
791



Sajal K. Das received his PhD in computer science in 1988 from the University of Central Florida, Orlando, FL. Currently, he is a Professor of computer science and engineering, and also the Founding Director of the Center for Research in Wireless Mobility and Networking (CReW-MaN) at the University of Texas at Arlington (UTA). Prior to 1999, he was the

faculty of computer science at the University of North Texas (UNT), Denton, where he served as the Director of the Center for Research in Parallel and Distributed Computing (CRPDC). Dr Das is a recipient of the UNT Student Association's Honor Professor Award in 1991 and 1997 for best teaching and scholarly research; UNT's Developing Scholars Award in 1996 for outstanding research; and UTA's Outstanding Senior Faculty Research Award in Computer Science in 2001. He has been a Visiting Scientist at the Council of National Research in Pisa and a Visiting Professor at the Indian Statistical Institute in Calcutta. His current research interests include mobile computing, wireless networks, QoS in wireless multimedia and mobile Internet, parallel algorithms, grid computing, performance modeling and simulation. He has published over 180 research papers in these areas, delivered numerous invited talks, directed several funded projects, and holds four US patents in wireless mobile networks. He received Best Paper Awards at ACM MSWIM 2000, MobiCom'99, and PADS'97. Dr Das serves as the Editorial Boards of JPDC, PPL, and PAA, and has guest-edited special issues of ACM Wireless Networks, JPDC, and IEEE Transactions on Computers. He served as General Chair of WoWMoM-2000 and PDC-WNMC-2001, General Vice-Chair of MobiCom-2000, HiPC-2000, and HiPC-2001, General Co-Chair of MASCOTS'98, Founding TPC Chair of WoWMoM'98 and WoWMoM'99, Program Vice-Chair of HiPC'99, and TPC member of numerous IEEE and ACM conferences. He is also a member of the IEEE TCPP Executive Committee.



Daniel J. Harvey received his PhD in computer science from the University of Texas at Arlington (UTA) in 2001. Currently, he is an Assistant Professor in the Department of Computer Science at Southern Oregon University, Ashland, OR. From 1992 to 2001, he was an Assistant Professor at Dallas Baptist University. He was nominated for the 2001 UTA Outstanding Doctoral Research Student Award. His re-

search interests include parallel programming, load balancing, and cluster computing. Dr Harvey has extensive experience in industry and was President of an automotive aftermarket value-added reseller for 13 years. He has considerable consulting experience working with firms such as Dunn & Bradstreet and Honeywell. In 1999, under a NASA summer grant, he conducted research at NASA Ames Research Center, Moffett Field, CA. He is also active in athletics, completing his fifth marathon at Boston in 1997. He established the Dallas Baptist University cross-country and track programs in 1996, and served as their Head Coach through 2001.



Rupak Biswas received his PhD in computer science from Rensselaer Polytechnic Institute, Troy, NY, in 1991, and is currently a Senior Computer Scientist with NASA Ames Research Center, Moffett Field, CA. In the past, he was a Senior Research Scientist with Computer Sciences Corporation and with Veridian/MRJ, and a Staff Scientist with the Research Institute for Advanced Computer Science (RIACS),

all at NASA Ames. He is the Group Lead of the Algorithms, Tools, and Architectures (ATA) Group that performs research in computer science technology for high-performance scientific computing. The ATA Group is part of the NASA Advanced Supercomputing (NAS) Division of NASA Ames. Dr. Biswas has published over 85 technical papers in journals and major conferences, given several invited talks at home and abroad, and guest-edited several journal special issues. He received the Best Paper Award for significant research contributions at Supercomputing'99, and the Best Student Paper Award at Supercomputing-2000. He was awarded the NASA Contractor Council Excellence Award in 1993 for his work on developing an automatic mesh adaptation procedure for unstructured meshes. He was a co-recipient of the 2001 NASA Group Achievement Award as a member of the information power grid (IPG) Group which made outstanding contributions to the agency's mission. His current research interests are in dynamic load balancing for NUMA and multithreaded architectures, analyzing and improving single-processor cache performance for irregular applications, scheduling strategies for heterogeneous distributed multi-resource servers in the IPG, and the scalability and latency analysis of key NASA algorithms and applications.

792
793
794
795
796
797
798
799
800
801
802
803
804
805
806
807
808
809
810
811
812
813

UNCORRECTED